Journal of Molecular Catalysis B: Enzymatic 113 (2015) 95–103

Contents lists available at ScienceDirect

Journal of Molecular Catalysis B: Enzymatic

journal homepage: www.elsevier.com/locate/molcatb

Hairy root mediated functional derivatization of artemisinin and their bioactivity analysis

Pallavi Pandey[a], Sailendra Singh[a], Nimisha Tewari[b], K.V.N.S. Srinivas[c], Aparna Shukla[d], Namita Gupta[e], Prema G. Vasudev[d], Feroz Khan[d], Anirban Pal[b], Rajendra Singh Bhakuni[f], Sudeep Tandon[g], Jonnala Kotesh Kumar[c,*], Suchitra Banerjee[a,*]

[a] Plant Biotechnology Division, Central Institute of Medicinal and Aromatic Plants (CSIR-CIMAP), Lucknow 226015, Uttar Pradesh, India
[b] Molecular Bioprospection Division, Central Institute of Medicinal and Aromatic Plants (CSIR-CIMAP), Lucknow 226015, Uttar Pradesh, India
[c] Natural Product Chemistry Division, Central Institute of Medicinal and Aromatic Plants (CSIR-CIMAP), Research Centre, Boduppal, Hyderabad - 500092, Telangana, India
[d] Metabolic and Structural Biology Division, Central Institute of Medicinal and Aromatic Plants (CSIR-CIMAP), Lucknow 226015, Uttar Pradesh, India
[e] Analytical Chemistry Division, Central Institute of Medicinal and Aromatic Plants (CSIR-CIMAP), Lucknow 226015, Uttar Pradesh, India
[f] Medicinal Plant Chemistry Division, Central Institute of Medicinal and Aromatic Plants (CSIR-CIMAP), Lucknow 226015, Uttar Pradesh, India
[g] Process Chemistry and Chemical Engineering Division, Central Institute of Medicinal and Aromatic Plants (CSIR-CIMAP), Lucknow 226015, Uttar Pradesh, India

ARTICLE INFO

Article history:
Received 12 September 2014
Received in revised form
24 December 2014
Accepted 13 January 2015
Available online 22 January 2015

Keywords:
Biotransformation
Artemisinin
Hairy root
Bioactivity
Molecular docking

ABSTRACT

Biotransformation of artemisinin (1) with the selected hairy root clones of three medicinally important plants, *i.e.*, *Atropa belladonna, Hyoscyamus muticus* and *Ocimum basilicum*, yielded two biotransformed products, which were identified as 3-α-hydroxy-1-deoxyartemisinin (2) and 4-hydroxy-9,10-dimethyloctahydrofuro-(3,2-i)-isochromen-11(4*H*)-one (3). Their structures were elucidated through spectroscopic analysis (NMR/MS) and X-ray crystallography. The relative transformation efficiencies of the tested hairy root clones differed concerning individual bioconversion reactions. Consequently, the HR clones of *H. muticus* and *A. belladonna* accomplished the highest conversion of (**1**) to (**2**) and (**3**) respectively, while that of *O. basilicum* imparted an intermediate response. *In-silico* and *in-vitro* bioactivity analysis of the derivatives revealed promising anti-plasmodial activity profile in tandem with notable TNF level lowering potential of compound (**2**), indicating thereby its prospective therapeutic merit in ameliorating the severity of malarial infection.

1. Introduction

Malaria ranks as one of the most alarming infectious parasitic diseases of the world and is imposing severe threat on approximately half of the global populations as per the existing WHO survey [1]. In spite of the tremendous worldwide research efforts to combat malaria, the global morbidity and mortality rates have not been ameliorated significantly over the last 50 years and re-emergence of malaria in many parts of the world is currently imposing fresh challenges due to rapid acquirement of drug-resistance by the parasite [2].

In general, the discovery of artemisinin, a sesquiterpene lactone containing an endoperoxide bridge and/or its analogues become increasingly popular as effective candidates of artemisinin-based combination therapy (ACT) for the treatment of drug-resistant malaria [3]. Although the ACT treatment regime showed reduction in the transmissibility of malaria by preventing gametocyte development [4], but delayed parasite clearance due to rapid emergence of artemisinin resistance [5] necessitated the discovery of new antimalarials with novel mechanism of actions [6].

Many efforts have been made to prepare simpler antimalarial molecules based on the trioxane ring of artemisinin or to produce semisynthetic and synthetic endoperoxides with greater metabolic and hydrolytic stability than artemisinin itself [7]. However, as the processes were complicated with low yields and high cost [8], efforts were diverted towards exploration of new avenues to produce more efficient artemisinin analogues or even new sesquiterpenes. Accordingly, the contemporary research findings corroborated the superior efficacies of artemisinin analogues for effective cancer chemotherapy (dihydroartemisinin) as well as in combination therapies for drug resistance malaria [3,9]. Currently

* Corresponding author. Tel.: +91 522 2718628; fax: +91 522 2342666.
E-mail addresses: koteshkumarj@yahoo.com (J.K. Kumar), suchitrabanerjee07@yahoo.com (S. Banerjee).

http://dx.doi.org/10.1016/j.molcatb.2015.01.007
1381-1177/

the WHO recommended antimalarial formulations that are being used as ACT consist of several artemisinin derivatives having long half-life than artemisinin, such as artemether-lumefantrine, artesunate-mefloquine, artesunate-amodiaquine, artesunate-sulfadoxine-pyrimethamine, dihydroartemisinin-piperaquine and arteether-curcumin [10–12].

Diversified efforts have been focused towards generating novel analogues either through combinatorial biosynthesis in microbes [8] or through bioconversion of artemisinin or its analogues (artemisinic acid, α and β artemether, arteannuin B) using microbial [13–18] and plant cell/tissue culture systems [16,19–22].

Judicious exploitation of the biotransformation proficiency of hairy root cultures (HR) is gaining world-wide attention due to the practical merit of this tool in generating novel products with widened bioactivities [23]. Besides possessing characteristically distinctive and coherent growth/enzymatic profiles, long-lasting operational stability and reduced cost involvement [24], HR cultures also enjoy the added benefits of inter-clonal variations in metabolic framework through the gainful assimilation of *Ri* T-DNA mediated insertional mutagenesis. Such attributes not only broadens the range of substrate adaptability but also modulate the regio and stereo-selective reaction specificity and thereby renders this system as a potent biotransformation tool in medicinal and therapeutic chemistry [25]. Several reports document the excellent biotransformation capabilities of hairy roots which consistently catalyze reactions in a stereospecific manner, resulting in chirally pure products [23,26]. It is however pertinent to mention that HR mediated biotransformation of artemisinin is less explored and till date only two reports of its conversion to deoxy derivative are available through the use of two different plant systems, *i.e.*, *Cyanotis arachnoidea* [27] and *Rheum palmatum* L. [28], which leaves ample scope for further exploration.

The necessity for identification of novel targets through diversity-based generation of molecules has already been unanimously acknowledged which can ideally combat the rapid emergence of parasite resistance [6]. Accordingly, the structural modifications of the functional groups of artemisinin holds much promise in fighting against drug resistance malaria. Under such circumstances, the accredited uniqueness of hairy root cultures in performing regio-specific modifications [26], which are otherwise arduous to carry out by microorganisms or synthetic chemical methods, further reiterates the potential of such exploration involving hairy roots of diverse plant systems with regard to artemisinin [23].

The present study explores the competence of the preselected elite HR clones of three medicinally important plants, *i.e.*, *Atropa belladonna, Hyoscyamus muticus* and *Ocimum basilicum*, for the biotransformation of artemisinin. This communication reports the first successful hairy-root mediated biotransformation of artemisinin (**1**) to 3-α-hydroxy-1-deoxyartemisinin (**2**) and 4-hydroxy-9,10-dimethyloctahydrofuro-(3,2-i)-isochromen-11(4*H*)-one (**3**), deduced through spectroscopic analysis (NMR/MS) and X-ray crystallography. During the present course of study, the *in-silico* and *in-vitro* bioactivity analysis of the derivatives revealed encouraging activity profile of compound (**2**) with respect to antiplasmodial activity coupled with notable TNF lowering potency.

2. Materials and methods

2.1. General experimental procedures

^{1}H, ^{13}C and 2D NMR spectra were recorded using Bruker Avance 300 MHz spectrometer and the chemical shifts (δ) were expressed in ppm with reference to TMS as internal standard. ESI–MS data were obtained on Shimadzu LC–MS system after dissolving compound in acetonitrile. IR spectra were measured by Spectrum BX Perkin Elmer and Spectronic® Genesys™, respectively.

2.2. Hairy root cultures

Two pre-selected hairy root clones of *A. belladonna* [29] and *H. muticus* [30] were used for the present study, which were maintained through sub-culturing in 1/2 strength Murashige and Skoog medium [31] supplemented with 3% sucrose (pH 5.88) and incubated with continuous shaking on a rotary shaker (80 rpm) at 25 ± 1 °C under dark condition. Additionally, one recently established hairy root clone of *O. basilicum*, having rapid growth potential and *rol* positive (both B and C) traits (data not presented), had also been utilized for the present biotransformation study following its maintenance under the aforesaid conditions.

2.3. Biotransformation procedures and Isolation of transformed products

The substrate (**1**), was dissolved in MeOH (40 mg/mL) and 1.0 mL of the solution was added to 50 mL of half-strength MS (3% sucrose) liquid media. These feeded media were dispensed in 2 weeks old hairy root cultures (~5.0 g FW) which were subsequently incubated at 25 ± 2 °C on rotary shaker (80 rpm) in dark. Two controls (substrate control and culture control) were also established, using MeOH instead of DMSO, following our previously reported protocol [26]. All the experiments were repeated thrice with three replicates for each category.

After co-incubation with the substrate, the cultures were harvested, the hairy root tissues were separated from the media and each were extracted with ethyl acetate in triplicates as per our earlier reported protocol [26]. The extracts were subjected to TLC analysis (silica gel 60 F_{254} Plate) using the optimized solvent systems (Diethyl ether: Hexane:: 7:3) followed by the UV detection at 254 nm and after spraying with anisaldehyde solution for visualization of the transformed products.

The time course study was performed in triplicate at weekly intervals (from 7 to 21 days) and quantification of the biotransformed products in both the media and HR tissues of all the three plant systems were carried out through HPTLC following our earlier reported method [29].

Consequently, for the isolation of the biotransformed products, the ethyl acetate extracts (250 mg) were subjected to column chromatography on silica gel (20 g, 60–120 mesh, 1 × 20 cm glass) and was eluted with increasing polarity mixture of ethyl acetate-hexane. The fractions collected in 5% ethyl acetate in hexane yielded compound (**2**) (48 mg), while that collected in 8% ethyl acetate in hexane gave compound (**3**) (22 mg). The structure of the isolated biotransformed products were elucidated by 1D/2D NMR, ESI–MS and further validated through X-ray crystallography.

2.3.1. 3-α-Hydroxy-1-deoxyartemisinin (*2*)

White crystalline solid; ^{1}H NMR ($CDCl_3$, 300 MHz) and ^{13}C NMR ($CDCl_3$, 75 MHz) see Table 1. ESI–MS 282.3.

2.3.2. 4-Hydroxy-9,10-dimethyloctahydrofuro-(3,2-i)-isochromen-11(4H)-one (*3*)

White crystalline solid; ^{1}H NMR ($CDCl_3$, 300 MHz) and ^{13}C NMR ($CDCl_3$, 75 MHz) see Table 1. ESI–MS 240.3.

2.4. X-ray crystallographic data

Single crystals of (**2**) were obtained by slow evaporation from chloroform/methanol mixture. Diffraction data were collected on Bruker AXS SMART APEX diffractometer using Mo

Table 1
^{1}H (300 MHz) and ^{13}C NMR (75 MHz) chemical shift data for compounds (**2**) and (**3**) in $CDCl_3$.

Assignment	Compound **2**			Compound **3**		
	^{1}H	^{13}C	Nature	^{1}H	^{13}C	Nature
1	1.66 (m, 1*H*)	41.00	CH	1.54 (m, *H*)	56.52	CH
2	1.65, 2.11 (m, 2*H*)	30.73	CH_2	1.43 and 1.88 (m, 2*H*)	27.28	CH_2
3	3.74 (bs, 1*H*)	69.48	CH	3.96, 4.15 (dd, 2*H*)	68.26	CH_2
4	–	109.29	Q	5.88 (br,1*H*)	110.66	CH
5	5.76 (s, 1*H*)	99.34	CH	–	86.88	Q
6	–	83.34	Q	1.95 (br, *H*)	48.33	CH
7	2.194 (m, 1*H*)	42.48	CH	1.45 and 2.03 (m, 2*H*)	26.84	CH_2
8	2.06 (m, 2*H*)	23.92	CH_2	1.96 (m, *H*)	35.37	CH_2
9	1.22, 1.95 (m, 2*H*)	33.80	CH_2	1.98 (m, *H*)	30.97	CH
10	1.434 (m, 1*H*)	35.53	CH	2.68 (m, *H*)	40.76	CH
11	3.325 (m, 1*H*)	33.10	CH	–	179.25	Q
12	–	171.72	Q	1.51 (d, 3*H*)	16.21	CH_3
13	1.322 (d, 3*H*)	12.96	CH_3	1.12 (d, 3*H*)	20.75	CH_3
14	1.06 (d, 3*H*)	18.77	CH_3	–	–	–
15	1.70 (s, 3*H*)	20.89	CH_3	–	–	–

*K*α radiation (λ = 0.7173 Å) in ω-scan mode at room temperature. Crystal data: $C_{15}H_{22}O_5$, *M* = 282.3, space group monoclinic, $P2_1$; unit cell dimensions were determined to be *a* = 5.464 (1) Å, *b* = 13.752 (2) Å, *c* = 9.845 (2) Å, β = 101.701 (7)°, *V* = 724.4 (2) Å^3, *Z* = 2, D_{calc} = 1.294 mg/m^3, *F*(0 0 0) = 304, μ(Mo *K*α) = 0.096 mm^{-1}; 2889 unique reflections were collected, of which 1510 reflections were observed on the basis of $F^2 > 4\sigma(F^2)$. The structure was solved by direct methods using SHELXS [32] and was refined against F^2 with full-matrix least squares method by using SHELXL [33]. All the non hydrogen atoms were refined anisotropically. Hydrogen atoms were fixed geometrically in idealized positions and were refined as riding over the atoms to which they were bonded. The final refinement gave *R* = 0.0521, R_w = 0.1032, goodness-of-fit, *S* = 0.943.

Crystals of (**3**) were obtained by evaporation from methanol. Diffraction data were collected at room temperature (293 K) on a Bruker Apex-II CCD diffractometer, using Mo *K*α radiation (0.71073 Å) in ω-scan mode. Crystal data: C13H20O4, *M* = 240.3, space group orthorhombic *P*212121; unit cell dimensions were determined to be *a* = 6.347 (7) Å, *b* = 12.002 (12) Å, *c* = 16.532 (16) Å, *V* = 1259 (2) Å3, *Z* = 4, Dcalc = 1.267 mg/m^3, *F*(0 0 0) = 520, μ(Mo *K*α = 0.093 mm^{-1}1; 2736 unique reflections were collected, of which 1308 reflections were observed with $F^2 > 4\sigma(F^2)$. The structure solution and refinement methods were similar as described for compound (**2**). The final *R* and R_w values were 0.0725 and 0.1637, respectively, with goodness-of-fit *S* = 1.159. Crystallographic data (excluding structure factors) of (**2**) and (**3**) have been deposited with the Cambridge Crystallographic Data Centre as supplementary publication numbers 1015578 and 1015579, respectively. Copies of the data can be obtained, free of charge, on application to CCDC, 12 Union Road, Cambridge CB2 1EZ, UK, (fax: +44 0 1223 336033 or deposit@ccdc.cam.ac.uk).

2.5. Molecular docking studies

Drawing and geometry cleaning of the studied compounds was performed through ChemBioDraw-Ultra-v12.0 software (http://www.cambridgesoft.com). The 2D structures has transformed into 3D structures using converter module of ChemBioDraw. The 3D structures then subjected to energy minimization. The docking study of selected target and ligand was done by using AutoDock Vina software (http://vina.scripps.edu/). The crystallographic structure of antimalarial target *Plasmodium falciparum* lactate dehydrogenase (pfLDH) (PDB ID: 1LDG) was retrieved through Brookhaven Protein Data Bank (PDB) (http://www.pdb.org). The valency and hydrogen bonding of the ligand as well as target protein was subsequently satisfied [34]. Polar Hydrogen atoms were added to the protein target to achieve the correct ionization and tautomeric states of amino acid residues such as His, Asp, Ser and Glu. Binding poses with the lowest docked energy belongs to the top-ranked cluster was selected as the final model for post-docking analysis with Discovery Studio v3.5, UCSF Chimera v1.5.3 (University of California, San Francisco) and PyMOL (The PyMOL Molecular Graphics System, Version 1.5.0.4 Schrodinger, LLC, USA).

2.6. In vitro antimalarial activity

2.6.1. Parasite cultures and treatment

Plasmodium falciparum (NF-54 strain) cultures were maintained as reported earlier [35]. Compounds (**1**) and (**2**) were solubilized in DMSO and further diluted with culture medium to achieve the required concentrations (final concentration of DMSO <1%). Parasite growth was determined spectrophotometrically in control and drug-treated cultures using a parasite lactate dehydrogenase assay (PfLDH). Chloroquine diphosphate salt was used as positive control. After incubation, plates were subjected to three 20 min freeze–thaw cycles to release cell content. Parasite culture was carefully mixed and aliquots of 20 μL were taken and added to another flat bottom 96-well plate containing 100 μL of Malstat reagent (0.125% Triton X-100, 130 mM L-lactic acid, 30 mM Tris buffer and 0.62 μM APAD) and 25 μL of NBT–PES (1.9 μM NBT and 0.24 μM PES) solution/well. The plate was incubated in dark for 30 min and absorbance was recorded at 650 nm using a microplate reader (FLUOStar Omega, BMG Labtech). All the experiments were done in triplicates. The antiplasmodial activity of the compound (**2**) was expressed as IC_{50} (mean ± SEM), calculated from dose-response curve data by nonlinear regression analysis.

2.6.2. Effect on suppression of TNF in murine peritoneal macrophages

Macrophages were collected from the peritoneum of mice injected with sterile 1% peptone and cultured as previously described [36]. The treatments with lipopolysaccharide (*Escherichia coli* 050: B5, Sigma, USA) at 1 μg/mL alone and in combination with compound (**2**) (1, 10 and 100 μg/mL) were accomplished for 18 h in triplicate. Tumor necrosis factor-α (TNF-α) activity in culture supernatants were estimated by Enzyme Immune Assay (EIA) using commercial kits for mouse TNF (BD Biosciences, USA).

3. Results and discussion

The HR clones of all the three tested plant systems revealed artemisinin (**1**) biotransformation competency and two derivatives, *i.e.*, (**2**) and (**3**), could be isolated, which were identified by

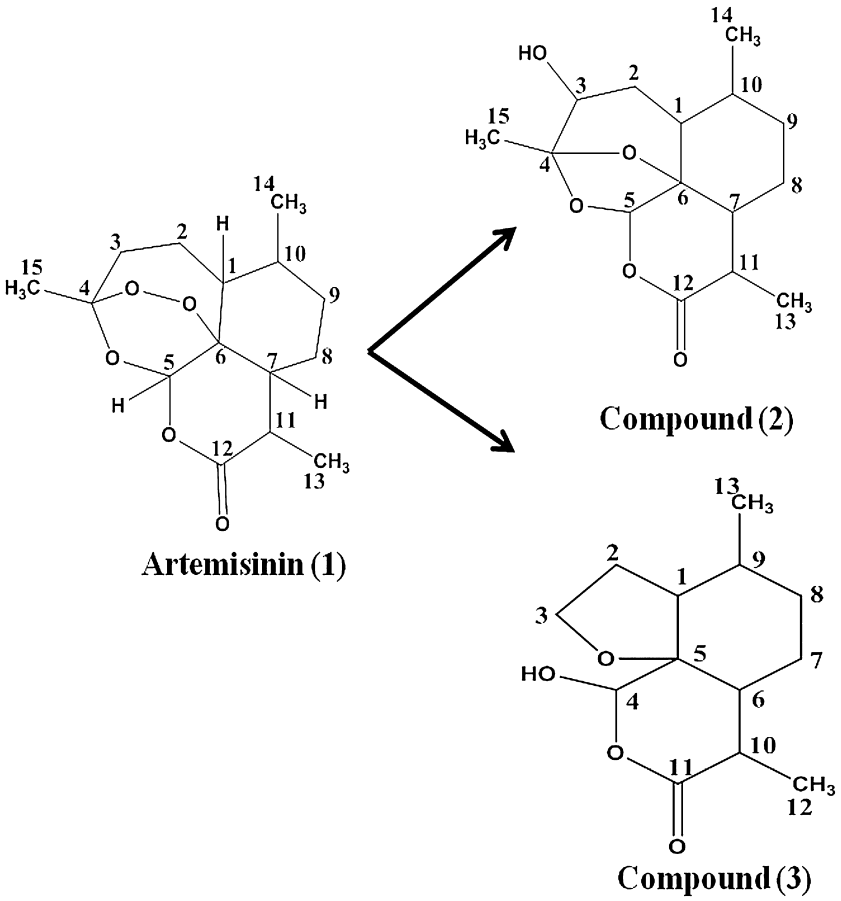

Fig. 1. Biotransformation of artemisinin (**1**) to 3-α-hydroxy-1-deoxyartemisinin (**2**) and 4-hydroxy-9,10-dimethyloctahydrofuro-(3,2-i)-isochromen-11(4*H*)-one (**3**) by the HR clones of *A. belladonna*, *H. muticus* and *O. basilicum*.

spectroscopy. None of the two controls demonstrated any such conversions of the substrate. The structures of the isolated compounds are represented in Fig. 1.

3.1. Identification of the biotransformed products

The structure elucidation of compounds (**2**) and (**3**), by various 1D and 2D NMR spectroscopy, revealed to be 3-α-hydroxy-1-deoxyartemisinin (**2**) and 4-hydroxy-9,10-dimethyloctahydrofuro-(3,2-i)-isochromen-11(4*H*)-one (**3**). Although, compound (**2**) was reported earlier in the *Artemisia annua* plant itself [37] as well as in various biotransformation studies [38], but compound (**3**) has resulted for the first time from the hairy root mediated biotransformation of artemisinin. The ^{13}C NMR (75 MHz) spectrum coupled with DEPT-135 showed that there are total 13 carbons in compound (**3**) of which two were quaternary, five tertiary, four secondary and two primary carbons (Table 1).

The two quaternary carbons were resonated at δ 179.25 (carbonyl carbon) and 86.88 ppm, respectively. The presence of a carbon resonance at δ 86.88 ppm was due to C-5 and this also suggests the absence of a peroxy bond in the structure. Also, presence of a carbon resonance at 68.26 ppm is attributed to C-3 and its germinal protons appearing at δ 3.96 and 4.15 ppm showed a long range correlation in HMBC spectrum with C-5 carbon confirms the ether linkage of the furan moiety in the structure. Presence of a down field resonance at δ 110.66 ppm is due to C-4 with a free hydroxyl attachment and this further confirms the absence of a seven membered lactone structure. Rest of the carbons were resonated as per the presently reported observation (Table 1).

Crystallization, followed by single crystal X-ray diffraction studies further confirmed the structures of (**2**) and (**3**). The crystal structure of (**2**) presented here is the same as that previously reported [38] (Supplementary Fig. S1a and b).

The molecular conformation of (**3**), obtained through single crystal X-ray diffraction, is depicted in Fig. 2a. The crystal structure confirmed the absence of a peroxide linkage and the presence of a tetrahydrofuran ring, as suggested by NMR analysis. An envelope conformation for the five-membered tetrahydrofuran ring and a stable chair conformation for the all-carbon 6-membered ring are observed in the crystal structure of (**3**). The other 6-membered ring containing lactone is flattened at O atom. An intermolecular hydrogen bond interaction between the O atom of the tetrahydrofuran ring and the hydroxyl group stabilize the molecular assembly in crystals (Fig. 2b; O3...O1 = 2.79 Å, H...O1 = 1.98 Å, ∠O3–H...O1 = 169.9°). The carbonyl O atom is involved in a weak C–H...O hydrogen bond interaction with the C6 (H) (Fig. 2b; C6...O2 = 3.25 Å, H6...O2 = 2.46 Å, ∠C6–H...O2 = 137°). Notably, the ring conformations observed for (**3**) are very similar to that observed for the O–acetyl derivative reported earlier [38]. However, the absence of a strong hydrogen bond donor like hydroxyl group has resulted in a different packing arrangement of the *O*-acetyl derivative crystals, in which a weak C–H...O hydrogen bond between the O atom of the five-member ring and the methyl hydrogen of acetyl group is observed.

3.2. Time course studies

The HPTLC analysis revealed that all the three tested HR clones displayed the maximum bioconversion of (**1**) to (**2**) on the 14th

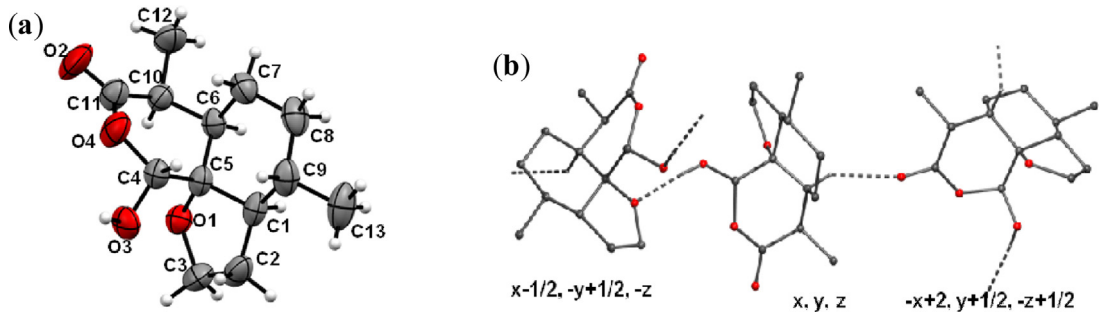

Fig. 2. (a) ORTEP drawing of compound (**3**) at 50% ellipsoid probability. (b) Intermolecular hydrogen bonds in the crystals of compound (**3**).

day of substrate feeding, although their relative efficiencies differed (Fig. 3a). The *H. muticus* HR clone performed best amongst the three (Fig. 3a) with regard to the conversion of (**1**) to (**2**) and displayed a maximum of >57% total conversion (*i.e.*, 49% in the medium and almost 8% in the hairy root tissue). On the other hand, the HR clones of *O. basilicum* and *A. belladonna* demonstrated comparatively lesser bioconversion potential (~3.2 and 5.7 times lower respectively). The HR clone of the former revealed a total of 18% conversion while that of the later displayed only 10% conversion of (**1**) to (**2**) after the same period of incubation. Microbial bioconversion of artemisinin to 3-α-hydroxy-1-deoxyartemisinin (**2**) by *Aspergillus niger* and two *Cunninghamella* species (*i.e.*, *C. echinulata, C. elegans*) had earlier

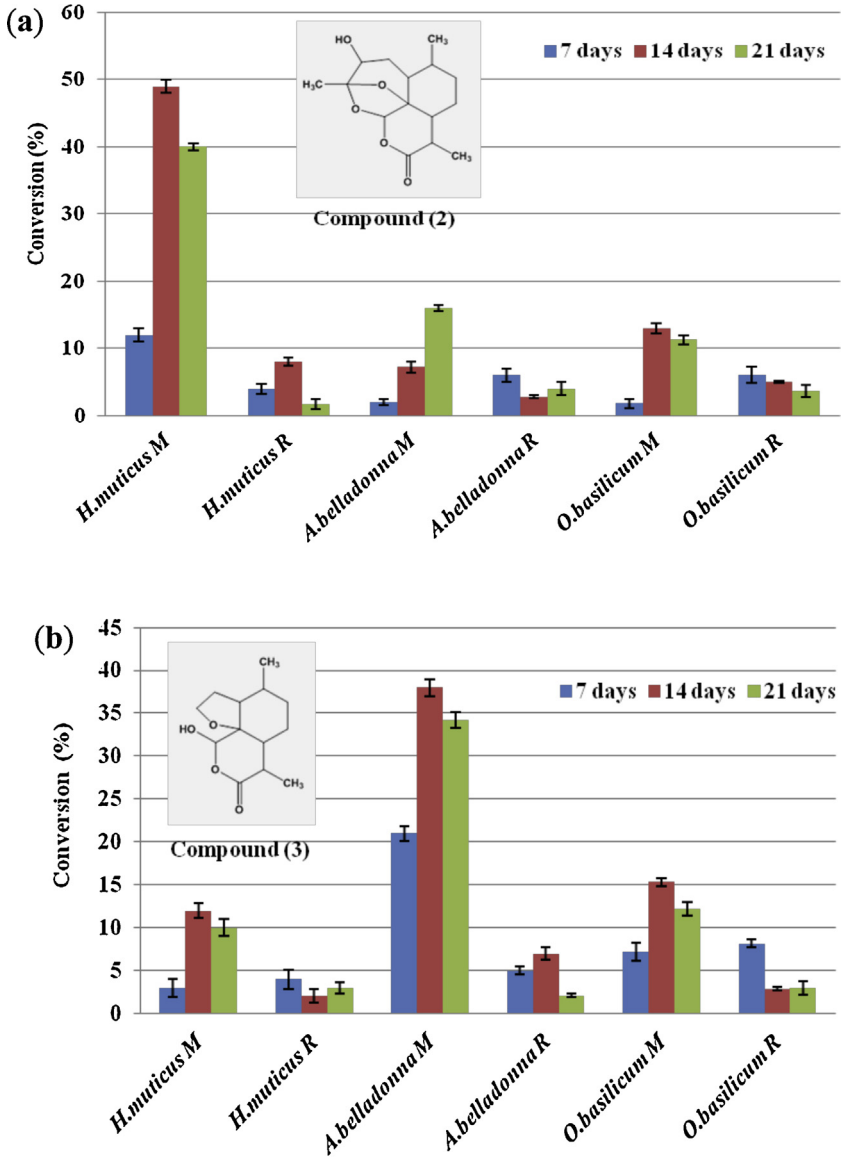

Fig. 3. Time course biotransformation proficiency analysis of the HR clones of different medicinal plants with regard to the conversion of artemisinin (**1**) to: (a) compound (**2**) and (b) compound (**3**) respectively, in the media and root tissues. (M-Media; R-Hairy root).

Table 2
Comparison of binding affinity of artemisinin and its derivatives (**2**) and (**3**) in terms of docking energy and binding site residues of anti-malarial target PfLDH (PDB: 1LDG).

Compound name	Binding energy (kcal mol^{-1})	Binding pocket residues (4 Å radius)	Key interacting residues and H-bonds
NADPH	−11.5	VAL-26, GLY-27, GLY-29, MET-30, ILE-31, PHE-52, ASP-53, ILE-54, VAL-55, MET-58, TYR-85, THR-97, ALA-98, GLY-99, PHE-100, THR-101, LEU-112, ASN-116, ILE-119, GLU-122, VAL-138, THR-139, ASN-140, VAL-142, LEU-163LEU-167, HIS-195, PRO-246, PRO-250	MET-30, ILE-31, ASP-53, ILE-54, TYR-85, ALA-98,GLY-99, PHE-100, VAL-138, ASN-140, LEU-163
Artemisinin	−7.7	PHE-52, ASP-53, ILE-54, TYR-85, ALA-98, GLY-99, PHE-100, ILE-119, ILE-123	ILE-54 (2 H-bonds 3.0, 3.5), GLY-99 (2 H-bonds 2.8, 2.9)
Compound 2	−6.3	GLY-27, SER-28, GLY-29, ASP-53, ILE-54, VAL-55, THR-97, GLY-99	ASP-53 (1.9), GLY-29 (3.1), THR-97 (2.9)
Compound 3	−5.6	GLY-29, ASP-53, ILE-54, VAL-55, MET-58, ALA-98, GLY-99, PHE-100	ASP-53 (2.1)

Note: The underlined residues of NADPH pocket participate in artemisinin and its derivatives (**2**) and (**3**) docking.

been reported with comparatively reduced conversion frequencies than that of the present findings [13,14]. On the contrary, none of the formerly reported plant cell/organ culture mediated biotransformation attempts of the substrate (**1**) had ever displayed similar bioconverted product formation [16,18–22,27,28].

Then again, the *A. belladonna* HR demonstrated the highest conversion efficiency with regard to the bioconversion of (**1**) to (**3**) after the same incubation period (14th day) and a maximum of >45% total conversion (*i.e.*, 38% in the medium and about 7% in the hairy root tissues) could be obtained (Fig. 3b). Likewise, the HR clones of *O. basilicum* and *H. muticus* also exhibited similar biotransformation response with decreased propensity as a total of 12% and 6% bioconversion of (**1**) to (**3**) were recorded respectively, which were ~3.75 and 7.5 times lower in that order than that with the *A. belladonna* HR mediated derivatization (Fig. 3b). To the best of our knowledge, similar conversion of (**1**) to (**3**) through the use of any biological systems has not been documented earlier and accordingly, the present observations corroborate special significance because of its exclusivity.

Apart from these two derivatives, (**1**) had also been converted by all the three tested HR cultures into a most prevalent derivative, *i.e.*, deoxyartemisinin at a lower proportion (~3 to 6%) as determined through HPTLC (Supplementary Fig. S2). The bioconversion

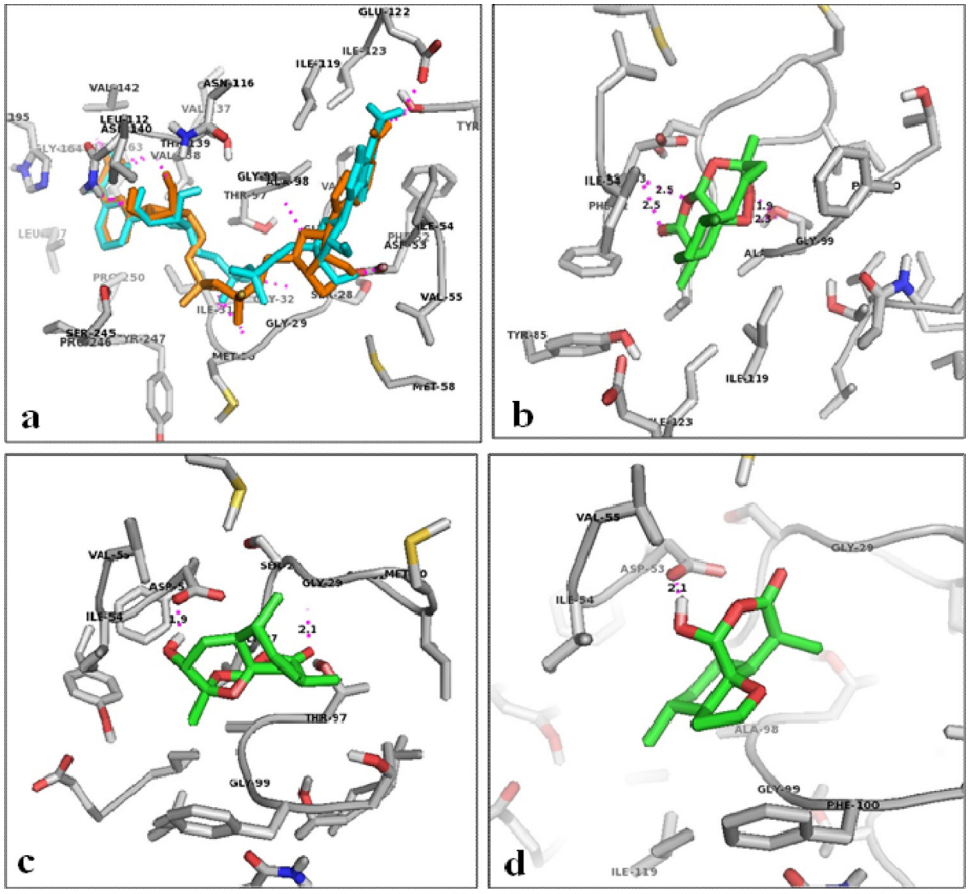

Fig. 4. Docking poses of artemisinin (**1**) and its derivatives (**2**) and (**3**) on PfLDH (PDB: 1LDG). (a) Docking procedure standardization by redocking of co-crystallized ligand NADPH with docking energy −11.5 kcal mol^{-1}, (b) Artemisinin (**1**) docked on PfLDH with binding energy −7.7 kcal mol^{-1}, (c) Compound (**2**) docked on PfLDH with binding energy −6.3 kcal mol^{-1} and (d) Compound (**3**) docked on PfLDH with binding energy −5.6 kcal mol^{-1}. *Note*: "H-bond is represented with magenta dashed line". (For interpretation of the references to color in this figure legend, the reader is referred to the web version of this article.)

Table 3
Comparison of binding affinity of artemisinin and its derivatives compound (**2**) and (**3**) in terms of docking energy and binding site residues of anti-inflammatory target TNF-α (PDB: 2AZ5).

Compound name	Binding energy (kcal mol^{-1})	Chain ID (dimer form)	Binding pocket residues (4 Å radius)	Interacting residues and length (Å)
Re-docking of bound inhibitor-307* in TNF-α dimer complex form	−9.6	Chain A	LEU-57, TYR-59, SER-60, TYR-119, LEU-120, GLY-121, GLY-122, TYR-151	–
		Chain B	LEU-57, TYR-59, SER-60, TYR-119, LEU-102, GLY-121TYR-151	
Artemisinin	−8.2	Chain A	TYR-59, TYR-119, LEU-120, GLY-121, TYR-151	–
		Chain B	TYR-59, TYR-119	
Compound 2	−7.9	Chain A	SER-60, TYR-119, LEU-120, GLY-121	GLY-121 (2.7), TYR-151 (3.0)
		Chain B	TYR-59, TYR-119, TYR-151	–
Compound 3	−7.5	Chain A	TYR-119, LEU-120, GLY-121, GLY-122	–
		Chain B	LEU-57, TYR-59, SER-60, TYR-119, TYR-151	

Note: "**–**" represent no H-bond and * refer TNF-α dimer inhibitor-307 named as (6,7-dimethyl-3-[(methyl{2-[methyl({1-[3-(trifluoromethyl)phenyl]-1*H*-indol-3-yl}methyl)amino]ethyl}amino)methyl]-4*H*-chromen-4-one).

of artemisinin to deoxyartemisinin have been well documented through the utilization of diverse biological systems, such as cell suspension [20,21] HR [27,28] and microbial cultures [15]. In all the three tested plant systems, the maximum recovery of the biotransformed products could be made from the media component (∼5–15 times higher than that in the HR tissues) and ethyl acetate was found to be the best solvent for the maximum recovery of the bioconverted products.

3.3. Molecular docking analysis

The docking of artemisinin (**1**) and its derivatives (**2** and **3**) was performed on PfLDH target enzyme (PDB: 1LDG), which demonstrated efficient binding to the NADPH binding site pocket (Table 2). The molecular docking prediction was evaluated by redocking of co-crystallized ligand NADPH on PfLDH, which showed high binding affinity docking energy *i.e.*, −11.5 kcal mol^{-1}. Results showed

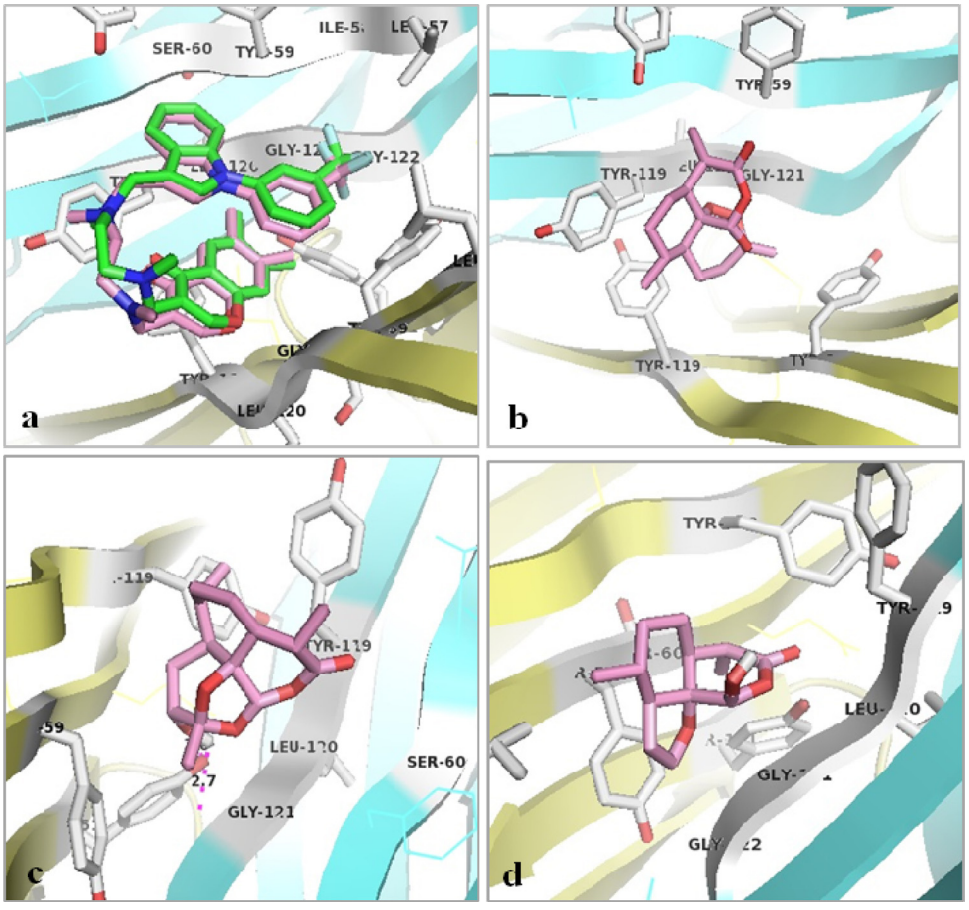

Fig. 5. Docking pose of artemisinin (**1**) and compound (**2**) and (**3**) on target TNF-α (PDB: 2AZ5). (a) Docking software standardization by redocking study of co-crystallized ligand 307* on 2AZ5 with docking binding energy −9.6 kcal mol^{-1}, (b) artemisinin (**1**) docked on TNF-α with binding energy −8.2 kcal mol^{-1}, (c) compound (**2**) docked on TNF-α with binding energy −7.9 kcal mol^{-1}, (d) compound (**3**) docked on TNF-α with binding energy −7.5 kcal mol^{-1}. *Note:* Ligand is highlighted in pink color, target chain A is highlighted in cyan color, target chain B is highlighted in yellow color and H-bond highlighted in magenta color. (For interpretation of the references to color in this figure legend, the reader is referred to the web version of this article.)

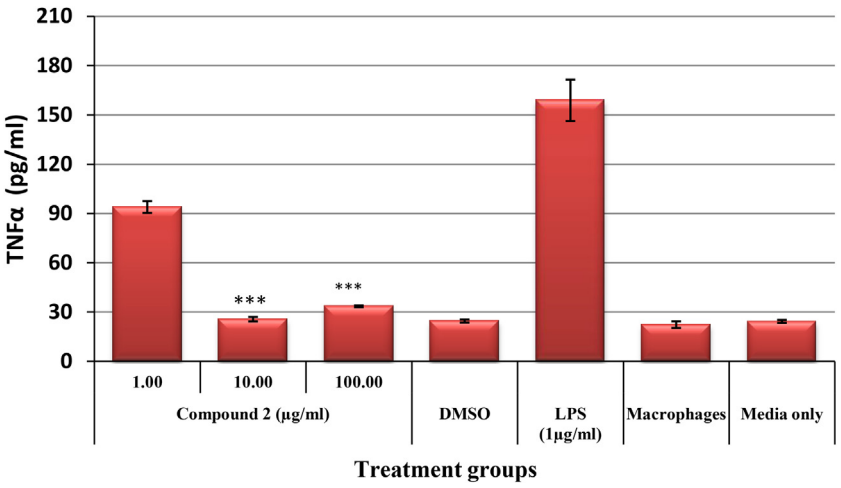

Fig. 6. Tumor necrosis factor-α (TNF-α) from the supernatant of macrophages cultured in the presence of compound (**2**). Peritoneal macrophages were stimulated with lipopolysaccharide (LPS) to produce TNF and treated with compound (**2**), solubilized in DMSO in a dose dependent manner, which at 10 and 100 μg/mL could significantly lower the level of TNF. MØ–Macrophages. *** = $p < 0.001$.

that the (**1**) docked well on pfLDH with high binding affinity docking energy of −7.7 kcal mol^{-1}, than the compound (**2**) (−6.3 kcal mol^{-1}) and compound (**3**) (−5.6 kcal mol^{-1}). The docked binding site residues of PfLDH for (**1**) within 4 Å region were PHE-52, ASP-53, ILE-54, TYR-85, ALA-98, GLY-99, PHE-100, ILE-119, ILE-123 and the H-bonds forming residues were ILE-54 (H-bond of 3.0 Å and 3.5 Å), GLY-99 (H-bond of 2.8 Å and 2.9 Å). Similarly, for compound (**2**), the docked binding site residues of PfLDH were GLY-27, SER-28, GLY-29, ASP-53, ILE-54, VAL-55, THR-97, GLY-99 and the H-bonds forming residues were ASP-53 (1.9 Å), GLY-29 (3.1 Å), THR-97 (2.9 Å) (Table 2). Likewise for compound (**3**), the docked binding site residues of PfLDH were GLY-29, ASP-53, ILE-54, VAL-55, MET-58, ALA-98, GLY-99, PHE-100 and the H-bond forming residue was ASP-53 (2.1 Å) (Fig. 4). The conserved residue was ASP-53, forming H-bonds in both binding sites.

Similarly, the docking of compounds (**1**), (**2**) and (**3**) was also performed on anti-inflammatory target-TNF-α (PDB: 2AZ5) (Table 3). Severe malaria has been associated with high TNF-α plasma levels, increased production of other cytokines (IFN-γ and IL-1β) and decreased production of anti-inflammatory cytokines. Pro-inflammatory Th1-type cytokines (*e.g.*, TNF-α, IFN-γ, interleukin IL-1β, and IL-6) are found critical for the control of exoerythrocytic and erythrocytic Plasmodium infection, but their increased production may also contribute to organ damage, particularly in the brain [39]. The clinical studies also demonstrated TNF to cause toxic side effects such as headache, nausea, vomiting, fever, chills and myalgia [40], which justifies for the selection of this cytokine as the target of the present docking studies. The docking protocol standardization was done by redocking study of co-crystallized ligand 307 (PDB: 2AZ5) on TNF-α dimer, which showed high binding affinity to the receptor with binding energy of −9.6 kcal mol^{-1}. Results showed that (**1**) docked well on TNF-α with docking binding energy −8.2 kcal mol^{-1}, consecutively followed by its derivatives: compound **2** (−7.9 kcal mol^{-1}) and compound **3** (−7.5 kcal mol^{-1}). The chemical nature of binding site residues of TNF-α dimer structural unit (Chain A and B) were aliphatic due to LEU-57, LEU-120, GLY-121, GLY-122 and aromatic due to TYR-59 and TYR-119. The hydroxyl group containing residue within the binding site was SER-60 (Fig. 5).

3.4. Biological activity evaluation

The *in-vitro* bioactivity analysis against *P. falciparum* revealed that the biotransformed compound (**2**) holds prospective anti-plasmodial activity of 31.88 ± 2.59 μM, corroborating the aforesaid *in-silico* predictions, wherein the docking energy is comparable to that of the parent compound (**1**). Moreover, the IC_{50} value of this compound (**2**) is comparable to that of our earlier reported natural molecule—glabridin [35], which has demonstrated anti-plasmodial activity having the IC_{50} value of 23.9 ± 0.43 μM with respect to the positive control—artemisinin (0.007 ± 0.004 μM).

Additionally, in agreement to the *in-silico* forecasting, the compound (**2**) has also been observed to significantly lower the levels of tumor necrosis factor, as determined through the *in-vitro* bioactivity analysis (Fig. 6). It has already been established that TNF and related cytokines initiate events that cause pathology, as well as parasite death within red cells in such infectious diseases [41]. Furthermore, TNF level has been clinically proven to rise in patients infected with *Plasmodium falciparum* [42]. TNF also activates a broad array of intracellular signal mechanisms triggering the inflammatory machinery within the host, through the NFKβ pathway [43]. Artemisinin derivatives, like artesunate have been reported to decrease the TNF levels, which in turn do not allow triggering the release of other pro-inflammatory cytokines, thus retarding the deterioration of body conditions [44]. The increase in TNF levels in malaria infected patients might also lead to secondary complications, like hypoglycaemia, which eventually deteriorates the prognosis of the disease [44]. In the background of such information, the presently observed credentials of the biotransformed compound (**2**) in terms of its anti-plasmodial activity coupled with significant TNF lowering competence, highlight the therapeutic potential of this biotransformed product in ameliorating the severity of malarial infection.

4. Conclusions

The present findings evidently elucidated that the unanimously recognized goal of generating novel target- based functional derivatives of artemisinin can be effectively achieved through such HR mediated derivatization of the parent molecule to cope with the impending emergence of drug resistance malaria. As per our knowledge, the present investigation records the first successful utilization of the HR clones of three different medicinal plants (*A. belladonna*, *H. muticus* and *O. basilicum*) to biocatalyze artemisinin into two atypical derivatives other than the most recurrently observed one (deoxyartemisinin). Rational exploitation of the biochemical machinery of hairy root clones to carry out such biotransformation reactions leading to the production of

artemisinin derivatives with interesting anti-malarial activity and TNF lowering competence can undoubtedly broaden the prospect of such research for future drug delivery.

Acknowledgement

The authors wish to express their sincere thanks to the Director, CSIR-CIMAP, for providing the facilities to carry out this research. Financial supports from Council of Scientific and Industrial Research and DST-SERB in the form of fellowships to PP, SS, NT and AS are also gratefully acknowledged. The work has been carried out under a CSIR-CIMAP in-house project (OLP-16).

Appendix A. Supplementary data

Supplementary data associated with this article can be found, in the online version, at http://dx.doi.org/10.1016/j.molcatb.2015.01.007.

References

[1] World Health Organization, World Malaria Report 2011, World Health Organization, Geneva, 2011.
[2] S.I. Hay, C.A. Guerra, A.J. Tatem, A.M. Noor, R.W. Snow, Lancet Infect. Dis. 4 (2004) 327–336.
[3] A. Martensson, J. Stromberg, C. Sisowath, M.I. Msellem, J.P. Gil, S.M. Montgomery, P. Olliaro, A.S. Ali, A. Bjorkman, Clin. Infect. Dis. 41 (2005) 1079–1086.
[4] P.J. Guerin, P. Olliaro, F. Nosten, P. Druilhe, R. Laxminarayan, F. Binka, W.L. Kilama, N. Ford, N.J. White, Lancet Infect. Dis. 2 (2002) 564–573.
[5] K. Na-Bangchang, K. Congpuong, Tohuku J. Exp. Med. 211 (2007) 99–113.
[6] S. Dandapani, E. Comer, J.R. Duvall, B. Munoz, Future Med. Chem. 4 (2012) 2279–2294.
[7] D.D. Begue, Bonnet, Drugs Future 30 (2005) 509–518.
[8] C. Liu, Y. Zhao, Y. Wang, Appl. Microbiol. Biotechnol. 72 (2006) 11–20.
[9] N.P. Singh, H.C. Lai, Anticancer Res. 25 (2005) 4325–4331.
[10] D. Sinclair, B. Zani, S. Donegan, P. Olliaro, P. Garner, The Cochrane collaboration, in: The Cochrane Library, 4, John Wiley & Sons, Ltd., UK, 2009, pp. 1–127, http://dx.doi.org/10.1002/14651858.
[11] P.G. Vathsala, C. Dende, V.A. Nagaraj, D. Bhattacharya, G. Das, P.N. Rangarajan, G. Padmanaban, PLoS ONE 7 (1) (2012) e29442, http://dx.doi.org/10.1371/journal.pone.0029442.
[12] R.N. Price, J. Infect. Dis. (2013) 1–3.
[13] J.-X. Zhan, Y.-X. Zhang, H.-Z. Guo, J. Han, L.-L. Ning, D.-A. Guo, J. Nat. Prod. 65 (2002) 1693–1695.
[14] I.A. Parshikov, B. Miriyala, K.M. Muraleedharan, A. Illendula, M.A. Avery, J.S. Williamson, Pharm. Biol. 43 (2005) 579–582.
[15] S. Srivastava, S. Luqman, A. Fatima, M.P. Darokar, A.S. Negi, J.K. Kumar, K. Shanker, Sci. Pharm. 77 (2009) 87–95.
[16] S.G. Musharraf, J. Uddin, M. Akhter, M. Parvez, S.S. Khan, S. Yousuf, S. Khan, M.I. Choudhary, J. Mol. Catal. B: Enzym. 82 (2012) 80–85.
[17] M.N. Omar, N.T. Khan, N.H.M. Hasali, S.F. Moin, H.Y. Alfarra, Adv. Biores. 3 (2012) 27–31.
[18] R. Gaur, S. Patel, R.K. Verma, A. Mathur, R.S. Bhakuni, Med. Chem. Res. 23 (2014) 1202–1206.
[19] S. Patel, R. Gaur, P. Verma, R.S. Bhakuni, A. Mathur, Biotechnol. Lett. 32 (2010) 1167–1171.
[20] S. Patel, R. Gaur, M. Upadhyaya, A. Mathur, A.K. Mathur, R.S. Bhakuni, J. Nat. Med. 65 (2011) 646–650.
[21] F. Sabir, A. Kumar, P. Tiwari, N. Pathak, R.S. Sangwan, R.S. Bhakuni, N.S. Sangwan, Z. Naturforsch. C (2010) 607–612.
[22] R. Gaur, S. Tiwari, A. Jakhmola, J.P. Thakur, R.K. Verma, R. Pandey, R.S. Bhakuni, J. Mol. Catal. B: Enzym. 106 (2014) 46–55.
[23] S. Banerjee, S. Singh, L.U. Rahman, Biotechnol. Adv. 30 (2012) 461–468.
[24] P. Pandey, R. Kaur, S. Singh, S.K. Chattopadhyay, S.K. Srivastava, S. Banerjee, Biotechnol. Lett. 36 (2014) 1523–1528.
[25] M. Kawauchi, T. Arima, O. Shirota, S. Sekita, T. Nakane, Y. Takase, M. Kuroyanagi, Chem. Pharm. Bull. 58 (2010) 934–938.
[26] V. Srivastava, R. Kaur, S.K. Chattopadhyay, S. Banerjee, Ind. Crops Prod. 44 (2013) 171–175.
[27] L.G. Zhou, D.C. Ruan, Z.D. He, H.T. Zhu, C.R. Yang, J.J. Wang, Acta Bot. Yunnanica 20 (1998) 229–232.
[28] L. Lixin, S. Yanfang, L. Xiaofeng, G. Dean, J. Chin. Pharm. Sci. 4 (2002) 122–124.
[29] V. Srivastava, A.S. Negi, P.V. Ajayakumar, S.A. Khan, S. Banerjee, Appl. Biochem. Biotechnol. 166 (2012) 1401–1408.
[30] M. Zehra, S. Banerjee, A.A. Naqvi, S. Kumar, Plant Sci. 136 (1998) 93–99.
[31] T. Murashige, F. Skoog, Physiol. Plant. 15 (1962) 473–497.
[32] G.M. Sheldrick, SHELXS-97, University of Gottingen, Gottingen, Germany, 1997.
[33] G.M. Sheldrick, SHELXL-97, University of Gottingen, Gottingen, Germany, 1997.
[34] G.M. Morris, D.S. Goodsell, R.S. Halliday, R. Huey, W.E. Hart, J. Comput. Chem. 19 (1998) 1639–1662.
[35] H.S. Cheema, O. Prakash, A. Pal, F. Khan, D.U. Bawankule, M.P. Darokar, Parasitol. Int. 63 (2014) 349–358.
[36] J. Agrawal, K. Shanker, D. Chanda, A. Pal, Parasitol. Res. 112 (2013) 2601–2609.
[37] C. Jing, Z. Yu-Bo, Z. Xin, H. Li, S. Wei, W. Jin-Hui, J. Shenyang Pharm. Univ. 25 (2008) 866–870.
[38] A.J. Lin, D.L. Klayman, J.M. Hoch, J. Org. Chem. 50 (1985) 4504–4508.
[39] P. Kinra, V. Dutta, Trop. Biomed. 30 (2013) 645–653.
[40] B. Beutler, D. Greenwald, J. Hulmes, M. Chang, Y. Pan, J. Mathison, R. Ulevitch, A. Cerami, Nature 316 (1985) 552–554.
[41] I. Clark, Cytokine Growth Factor Rev. 18 (2007) 335–343.
[42] P. Tangteerawatana, S. Krudsood, N. Kanchanakhan, M. Troye-Blomberg, S. Khusmith, J. Trop. Med. Public Health 45 (2014) 517–530.
[43] H. Xu, Y. He, X. Yang, L. Liang, Z. Zhan, Y. Ye, X. Yang, F. Lian, L. Sun, Rheumatology 46 (2007) 920–926.
[44] K. Elased, J. Taverne, J. Playfair, Clin. Exp. Immunol. 105 (1996) 443–449.